Oxidation of Ti–6Al–4V alloy between 450 and 600°C. Evolution of microstructure and mechanical properties.

Dominique Poquillon[1], Coralie Parrens[1] Alessandro Pugliara[1,2], Maxime Perrais[1], Benoit Malard[1]

[1] CIRIMAT, Université de Toulouse, France

[2] UMS Castaing, Université de Toulouse, France

Corresponding author: dominique.poquillon@ensiacet.fr

Abstract

Titanium alloys are widely used in many applications thanks to their good corrosion resistance and to their high specific modulus. However, at temperatures above 450°C, oxidation must be taken into account to improve life assessment of components. Especially for long-term exposures, oxidation leads to an oxide scale along with an oxygen enrichment in the metal below this oxide scale. In this study, the oxidation behaviour of Ti–6Al–4V is investigated between 450 and 600°C for a maximum duration of about 6800 h. Scanning electron microscope (SEM) and transmission electron microscopy (TEM) are used to characterize the oxide layer and the layer affected by oxygen uptake. The local oxygen content is quantified. Vibration tests are performed to determine elastic properties on thin specimens with different thicknesses affected by oxygen enrichment. Creep tests are also carried out to quantify the influence of this oxygen uptake on viscoplastic behaviour. An oxygen-enriched zone occupying 5% of the cross-section of a specimen is sufficient to induce detectable changes in its creep behaviour.

1. Introduction

Titanium alloys have long been used in aeronautical applications [1-3], but despite their high melting temperature, they are limited in their operating temperatures [4]. Their oxidation kinetics but especially the significant modification of the sub-surface microstructure due to their oxygen (or even nitrogen) enrichment penalizes their durability in applications above 500°C [5].

Thus, increasing turboreactor performance requests to increased temperatures and to decrease components mass. That is the reason why Titanium-aluminide (TiAl) blades have been chosen on the low-pressure turbine of the recent CFM International LEAP engine. However, titanium alloys remains economically and mechanically efficient for a wide range of applications due to its excellent corrosion resistance, very good specific rigidity and the possibility of manufacturing components by many conventional processes and also by additive manufacturing processes [6-7]. As Ti–6Al–4V is the most widely used titanium alloy, it was chosen for this work.

Many studies have been devoted to their limitations in applications on tribological [8-9], fatigue and ageing aspects [10-16]. We focus here on static loadings (creep behaviour) on samples in which oxidation affects only a small proportion of the section, as the sensitivity of titanium alloys to strain rate effect is well known [17-20].

2. Material and experiments

The material used for this study was provided by TITANIUM SERVICES. It is a 1 mm thick Grade 5 Titanium sheet. In the manual polishing, SiC paper grit, 600 and 1200 have been used successively. Fig. 1 shows the bimodal microstructure of the material used. The alpha grains are homogenous and equiaxed.

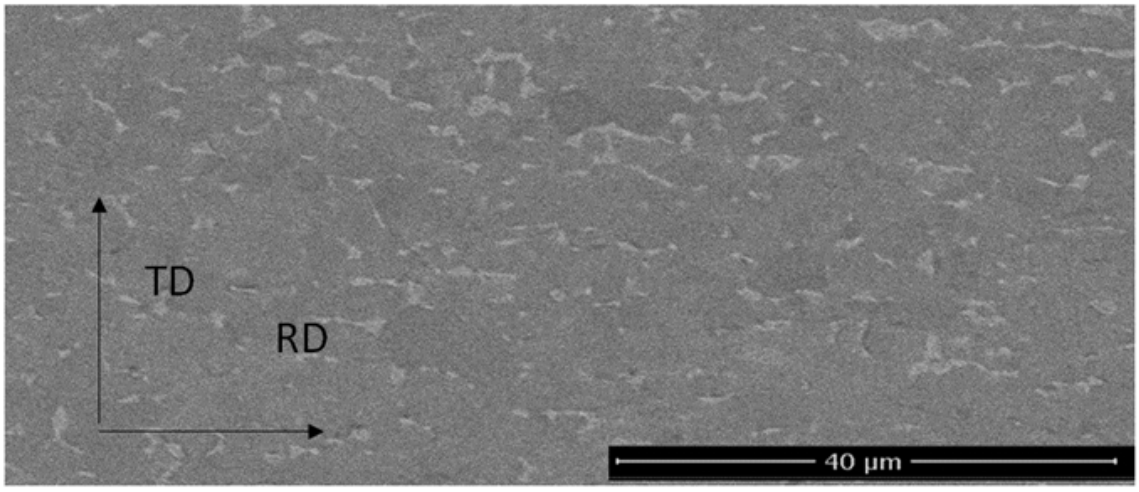

Fig. 1: Optical microscope observation of the Ti–6Al–4V microstructure etched with Kroll's reagent.

Oxidations were carried out in a Carbolite furnace, out under laboratory air, at 450 to 600°C for periods ranging from 8 to 6800 hours. Samples (20 x 10 x 1 mm^3) have been weighed three times with the ultra-microbalance Sartorius balance whose accuracy was 20 mg before and after oxidation. Optical observations have been performed with the optical microscope (OM) Nikon MA200, SEM observations with a LEO435. The hardness profile used to identify the hardened layer has been carried out with a micro hardness Buelher using a 10 g mass and a Knoop indenter. At least 20 measurements have been proceed in the area of interest.

Some additional investigations have been carried out at The Raimond Castaing Microanalysis Centre for oxygen measurements on cross section using electron probe microanalyser (EPMA) CAMECA SXFive microprobe. Focused ion beam (FIB) sample preparation have been processed for the less oxidized samples with dual beam FIB/SEM FEI NanoLab HELIOS 600i and TEM observations have been performed with transmission electron microscope JEOL JEM-2100F equipped with an Energy Dispersive X-ray Spectroscopy (EDS) analyser (Brucker SDD Xflash 5030T) coupled with Scanning Transmission Electron Microscopy (STEM) detector (JEOL).

Resonant Frequency & Damping Analyser (RFDA) tests have been carried out by AUROCK C^{ie}. The RFDA test rig was used to do impulse excitation measurements on beams (10 x 40 x 1 mm^3), from room temperature up to 650°C under air. The purpose was to measure, with high accuracy, resonant frequencies of samples to calculate an equivalent Young's modulus [ASTM E 1876, ISO 12680-1, ENV 843-2]. Two heating cycles were performed, rising to 550°C at 3°C per minute, cooling and then rising to 650°C again at 3°C per minute.

The specimens which have been used for the creep mechanical tests have a standard flat geometry. They have been machined by electrical discharge along the rolling direction. Then, they are carefully polished, removing a least 50 µm on each side to limit effects due to machining. The section of the sample in the gauge length was 3 mm^2 and the gage length was 36 mm. The total length of the creep sample, including enlarged shoulders was 72 mm. The thermal treatment of the samples devoted to creep test have been fitted on after the results of the oxidation tests detailed below. Creep tests were performed at 500 and 550°C under laboratory air on a creep testing device equipped with a ×20 balancing arm. For all the creep tests, the displacement was measured without contact through a high speed laser scanner to measure the spacing between reflective tape strips spot welded on the sample. The tests were always stopped before 5 % of creep strain to limit the risk of strain localization. The heating rate to the target temperature was set to 30 K/min. Two thermocouples spot welded on the sample heads showed a maximum temperature difference of 7 K.

3. Results

3.1 Oxidation kinetics and oxygen diffusion zone beneath the oxide scale

In this part of the study, the objective was to verify that in the tested time-temperature range, the oxidation kinetics could be described by a parabolic law [4]. The longest oxidation tests were conducted at 450° because there are fewer data in the literature at this temperature.

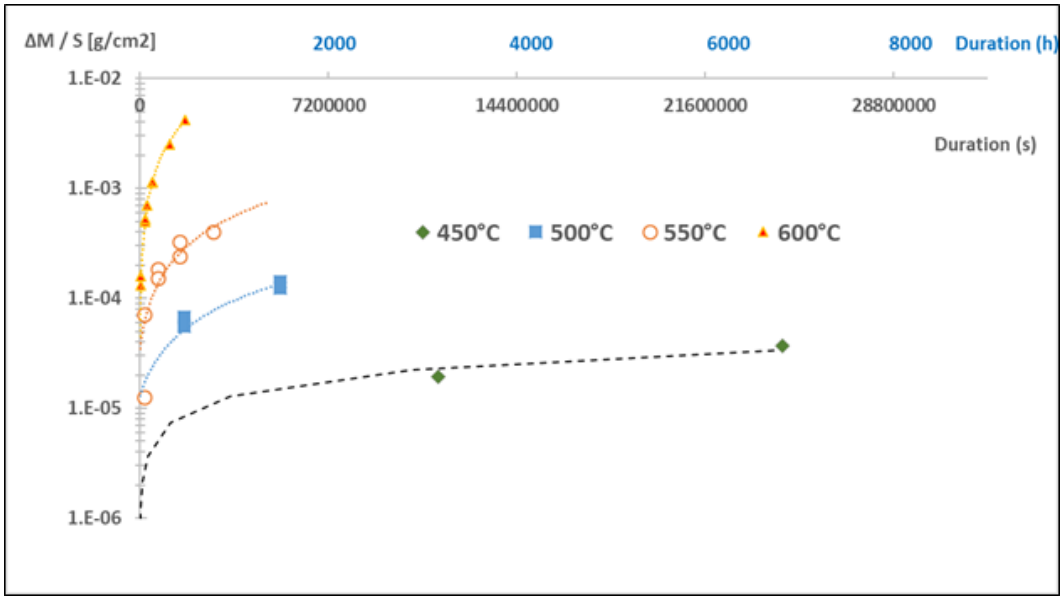

Fig. 2: Oxidation kinetics under laboratory air.

The figure 2 is a synthesis of the experiments carried out. A parabolic law can fit each curve for the 4 temperatures tested. The k_p values (Respectively 1.2 10^{-10} mg^2 cm^{-4} s^{-1} at 450°C, 2.8 10^{-9} mg^2 cm^{-4} s^{-1} at 500°C, 6.1 10^{-8} mg^2 cm^{-4} s^{-1} at 550°C and 4.1 10^{-7} mg^2 cm^{-4} s^{-1} at 600°C) are in good agreement with previous studies on alpha or near alpha titanium alloys [4, 5, 21]. After oxidation experiments, cross-sections have been prepared for hardness tests (Fig. 3). The purpose was to identify the affected depth and compare it to Castaing EPMA. At 600°C, following previous validated and published method [22-25], it was then possible to identify an effective diffusion coefficient of oxygen in the metal (7.6 10^{-17}. $m^2.s^{-1}$) in very good agreement with previous data [25]. At 550°C, longest oxidations are required to consolidate the first data obtained as the diffusion zone was too thin to perform hardness profile.

In the temperature range tested, no nitrogen enrichment has been evidenced contrary to what is reported for higher temperature [5].

For samples tested at 450°C, cross sections have been prepared using FIB/SEM. The oxide thickness was then measure for an average value of 170 nm after 6816 h of oxidation. The thickness for the sample oxidized 3168 h was around 130 nm but more difficult to measure due to surface roughness. For these two samples, the EDS resolution in the SEM was not sufficient to detect an oxygen profile below the oxide scale.

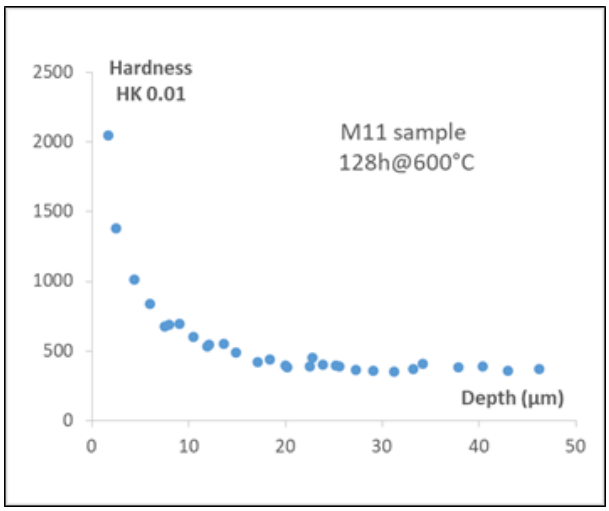

Fig. 3: Hardness profile after oxidation (128h at 600°C) under laboratory air.

However, a TEM cross-sectional preparation using FIB has been carried out for the M1 sample (471 h at 500°C). To avoid the possible oxygen contamination of TEM thin foil, this cross-sectional sample was immediately observed thanks to a JEOL JEM-2100F. The average oxide thickness was 240 nm. However, the oxide layer had a protuberance two to three times higher over the grain boundaries observed on the sample. Chemical analyses were performed using EDS on the TEM thin foil. Several profiles were made showing, under the oxide layer, a gradient of oxygen concentration over a depth of 1.8 mm so inside the first grain (Fig. 4). The oxygen value of each point of the profile shown in figure 4 is integrated along a line of 2 µm parallel to oxide layer. No oxygen enrichment on the grain boundaries was evidenced.

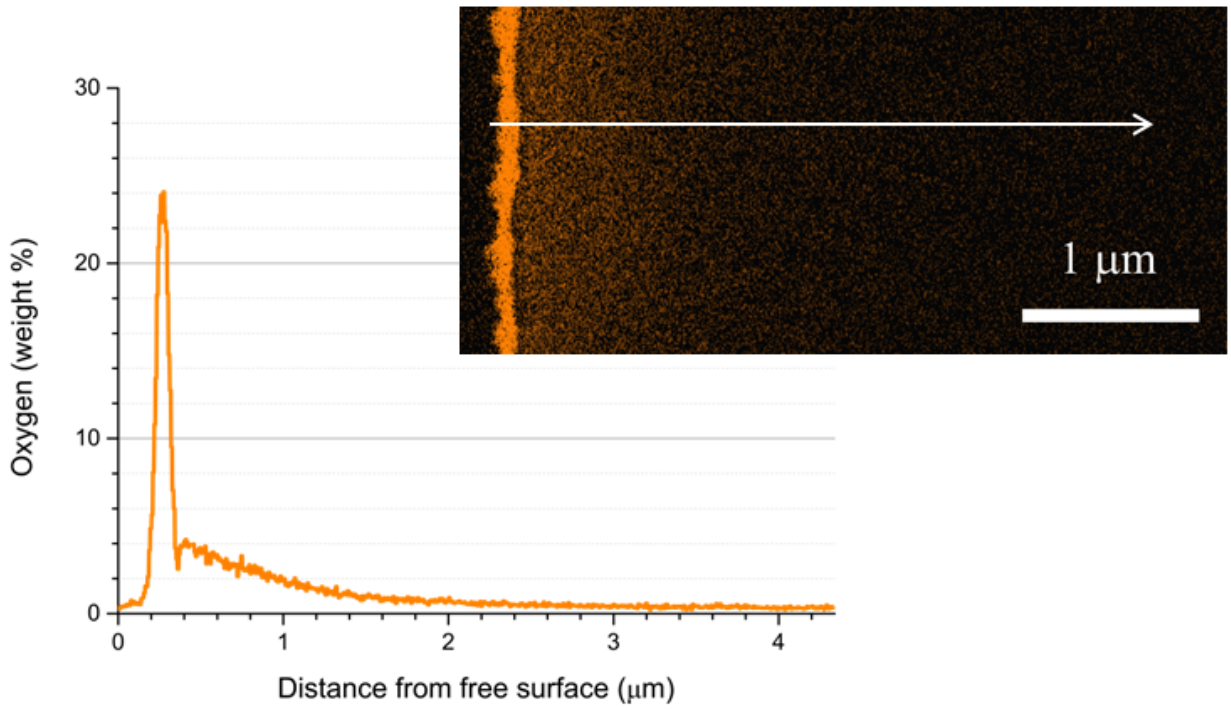

Fig. 4: TEM characterisation of sample M1 (471 h @ 500°C). STEM-EDS analyse on FIB cross-sectional sampling: a) oxygen profile; b) oxygen map.

Then, to carry out creep tests, we have chosen a single preoxidation condition (144 h at 600°C) for all creep tests in order to have a proportion of 5% of the cross-section affected by oxygen enrichment. The oxygen diffusion depth is then 18 mm. The selected conditions (temperature / oxidation duration) ensure that there is no detectable change in the core microstructure of the thin samples (thickness is below 1 mm), that an oxygen gradient is created from the surface and that the thin oxide scale remains adherent.

3.2 RFDA tests.

These tests are standardized and usually used for homogeneous samples. This is the case for the as received specimen but not for those that have been pre-oxidized. The test allows us to have, at different temperatures, the natural frequency of the longitudinal vibration of the beam. A formula is then used to calculate the longitudinal Young's modulus of the material tested. For specimens that are not homogeneous (due to the oxygen gradient), it is more appropriate to say 'Equivalent Young's modulus' (E_{eq}). For all tests performed, the E_{eq} decrease with temperature is linear from 20 to 650°C (Fig. 5a). The proportion of the area enriched in oxygen varies from 0.4% to 5% depending on the heat treatment conditions. This is

significantly lower than those previously tested [24, 25]. However, it can be seen in Fig. 5b that E_{eq} seems to increase with the depth of the affected area. However, further testing is needed to refine a proportionality law.

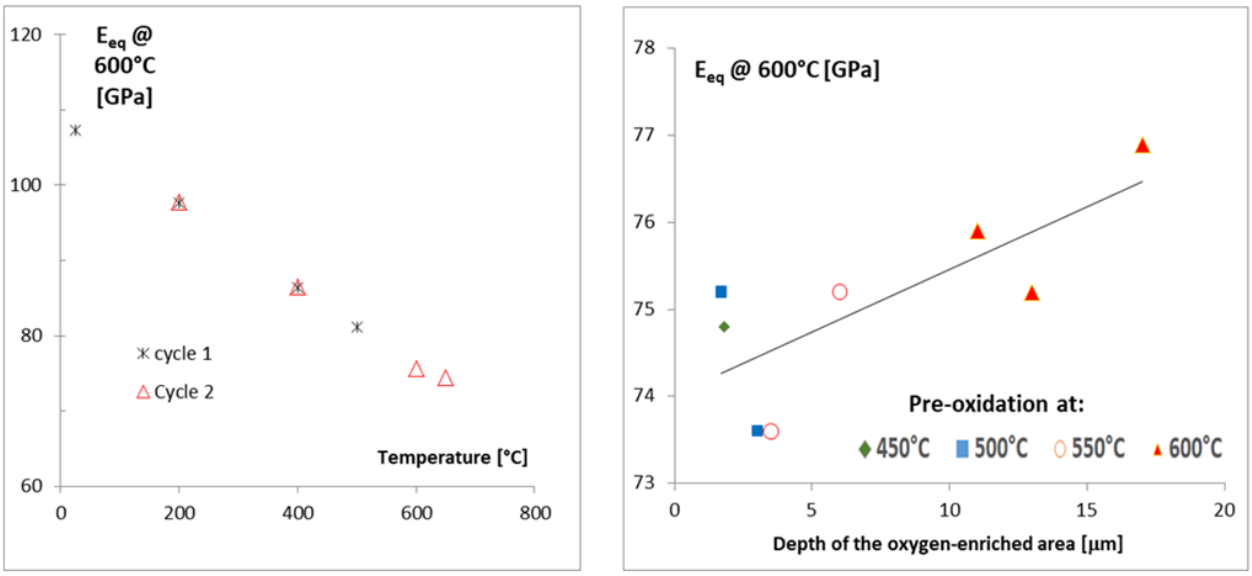

Fig. 5: a) RFDA test results for Sample A10 pre-oxidized 128h at 600°C b) RFDA results at 600°C: Equivalent Young's modulus for different oxidation conditions and oxygen uptake.

3.3 Creep tests

Creep test with increasing step loads have been carried out at 550 and 500°C on as-received samples and on pre-oxidized samples. The figure 6 illustrates the effects of preoxidation on the creep rate. For the all tested conditions, the creep rate is reduced on pre-oxidized samples. This is due to a core shell effect as the rigidity of the oxygen-affected zone (shell) increases, the net stress in the core of the sample decreases. This effect has been studied previously in other titanium alloys [22 - 25].

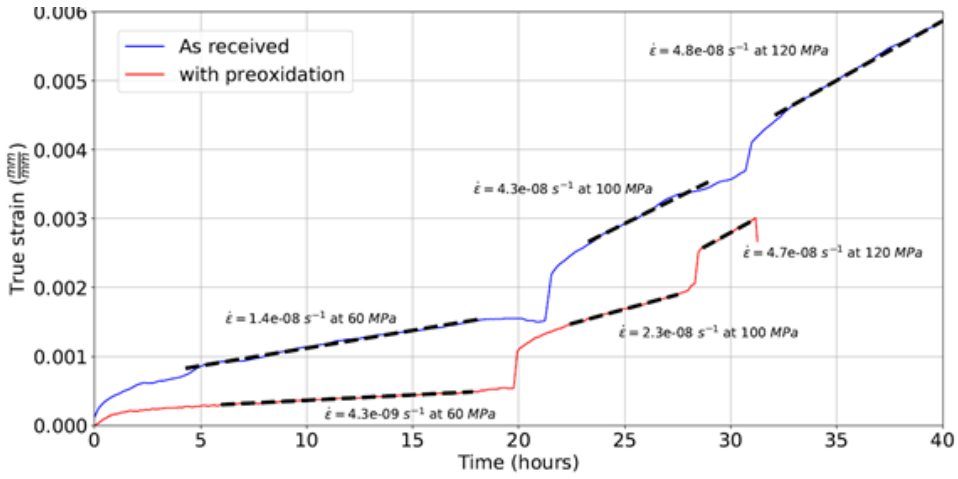

Fig. 6: Creep tests on as-received and pre-oxidised samples at 500°C.

A Norton plot on the figure 7 summarized the data obtained in this study. The creep strain rate seems to be more reduced for the lower stresses and new experiments are on-going to confirm that. However, this effect remains beneficial (by decreasing the overall apparent creep rate) as long as cracks initiated in the oxide scale do not propagate into the metal. Interrupted creep tests for small strain (1%) do not show any crack penetration into the alloy.

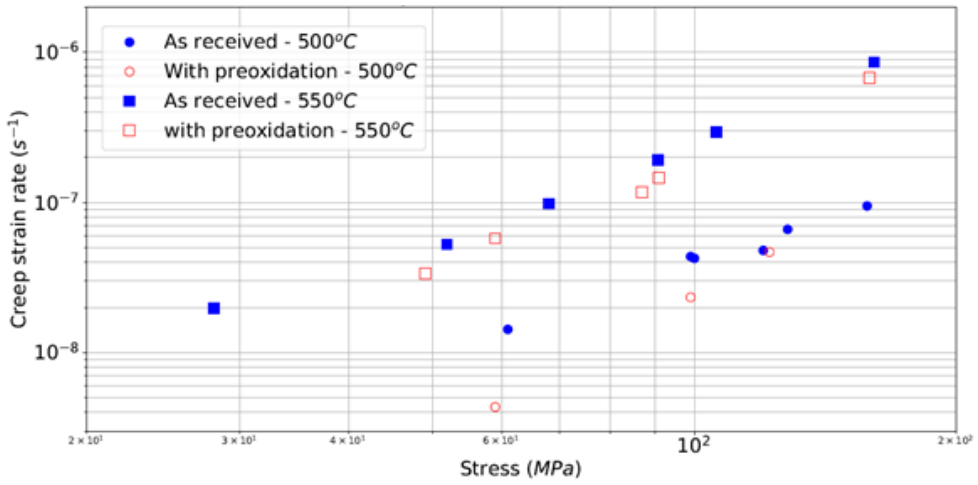

Fig. 7: Norton plot summarizing all the creep tests carried out on as-received and pre-oxidised samples at 500 and 550°C.

4. Conclusion and perspective

Several authors reported that some oxygen additions can enhance mechanical properties of titanium, such as tensile and fatigue strengths but only for limited addition not to compromise toughness and ductility [1-3]. Strengthening structural alloys with the addition of solute atoms is wildly used. For titanium alpha or near alpha alloys, the lattice parameters a and c of alpha-titanium increase with the local oxygen content [22-23] as well as the Young Modulus [24]. However few studies have been devoted to understand the effect of oxygen on plasticity at the atomic scale. Recently, Yu and co-workers [26] by using TEM and nanomechanical characterization report that the intense hardening effect of dilute oxygen solutes in pure alpha-Ti is due to the interaction between oxygen and the core of screw dislocations that mainly glide on prismatic planes. For aeronautical components such as fairing, covers that are moderately mechanically loaded but operate in areas where oxidation is not negligible, it is interesting to question the gain thus obtained in service and even the positive effect of a short initial preoxidation.

However, it is important to check whether during anisothermal creep tests, i.e. in thermal cycling with constant load, the beneficial effect remains. Tests are planned to check this point. The fatigue strength of titanium alloys has been the subject of numerous publications [1, 19, 27-31] but the vast majority of these tests have been conducted at room temperature. Fewer studies have been conducted on the fatigue strength of titanium alloys above 400°C [10, 12, 32- 35] and the effects of oxidation on dwell time when coupling between phenomena occurs requires experimental studies.

5. References

1. C. Leyens and M. Peters, Titanium and Titanium Alloys. Wiley-VCH, 2003
2. M. Peters, J. Kumpfert, C. H. Ward, and C. Leyens, ADV ENG.MATER, 2003, 5(6), 419–427
3. Y. Prasad, T. Seshacharyulu, MAT SCI ENG A-STRUCT, 1998, 243(1-2), 82-88
4. P. Kofstad, P. B. Anderson, and O. J. Krudtaa, J. LESS COMMON MET, 1961, 3(2), 89–97
5. C. Dupressoire, A. Rouaix-Vande Put, P. Emile, C. Archambeau-Mirguet, R. Peraldi, D. Monceau, OXID MET, 2017, 87(3-4), 343-353
6. H. Attar, S. Ehtemam-Haghighi, D. Kent, X. Wu, M. Dargusch, MAT SCI ENG A-STRUCT, 2017, 705, 385-393
7. B. Dutta, S. Froes. In Titanium powder metallurgy (pp. 447-468). Butterworth-Heinemann, 2015
8. K. Aniołek, M. Kupka, A. Barylski, WEAR, 2016; 356, 23-29.
9. K. Farokhzadeh, & A. Edrisy, TRIBOL INT, 2016, 94, 98-111
10. H. Ghonem & R. Foerch, MAT SCI ENG A-STRUCT, 1991, 138(1), 69-81
11. A. Madsen, E., Andrieu, H. Ghonem, MAT SCI ENG A-STRUCT 1993, 171(1-2), 191-197
12. S. Hardt, H. Maier, H. Christ, INT J FATIGUE, 1999, 21(8), 779-789
13. L. Sasaki, G. Hénaff, M. Arzaghi, P. Villechaise, J. Delfosse, MAT SCI ENG A-STRUCT, 2017, 707, 253-258.
14. S. Hémery, P. Villechaise, SCRIPTA MATER, 2017, 130, 157-160.
15. S. Hémery, L. Signor, P. Villechaise, METALL MATER TRANS A, 2018,, 49(6), 2048-2056.
16. M. Dehmas, R. Katemi, B. Appolaire, E. Aeby-Gautier, B. Denand, B., S. Audion, In Proceedings of the 12th World Conference on Titanium 2011 (pp. 719-723).
17. H. Vigié, T. De Paula, M. Surand , B. Viguier, SOLID STATE PHENOM, 2017, 258, 570-573
18. M. Surand, Etude de la viscoplasticité en traction et en fluage de l'alliage TA6V de 20°C à 600°C, PhD., Toulouse INP, 2013.
19. V. Doquet, V. Greef, INT J FATIGUE, 2012, 38, 118-129
20. B. Barkia, V. Doquet, J., Couzinié, I. Guillot, MAT SCI ENG A-STRUCT, 2015, 624, 79-89
21. D. Poquillon, C. Armand, J. Huez, OXID MET, 2013, 79, 249-259
22. J. Baillieux, D. Poquillon, B. Malard, PHIL MAG LETT, 2015, 95(5), 245-252
23. J. Baillieux, D. Poquillon, B. Malard, J APPL CRYSTALLOGR, 2016, 49(1), 175-181
24. J. Baillieux, C. Archambeau, P. Emile, D. Poquillon, D. In Proceedings of CFM 2015. AFM Eds.
25. J. Baillieux. Effet de l'oxydation sur le comportement mécanique de structures minces en alliages de titane, PhD., Toulouse INP, 2015.
26. Q. Yu et al. SCIENCE , 2015, 347(6222), 635-639
27. J. Robinson and C. Beevers, MET SCI J., 1973,7, 153-163, 1973
28. G.R. Yoder, L.A. Cooley, T.W. Crooker, METALL MATER TRANS A, 1977, 8, 1737-1752,

29. T.W. Duerig, J.E. Allison, J.C. Williams. METALL MATER TRANS A,1985, 16 , 739-749
30. P. Lefranc, C., Sarrazin-Baudoux, V. Doquet, J. Petit. SCRIPTA MATER, 2009, 60(5), 281-284
31. L.Yang, J. Liu, J.Tan, Z. Chen, Q. Wang, R. Yang, J MATER SCI TECHNOL, 2014, 30(7), 706-709, 2014.
32. R. Foerch, A. Madsen, H. Ghonem. 0. METALL MATER TRANS A, 1993, 24(6), 1321-1332
33. P. Pototzky, H. J. Maier, H. J. Christ, METALL MATER TRANS A, 1998, 29(12), 2995-3004
34. H. Ghonem. INT J FATIGUE, 2010 32(9), 1448-1460
35. D. P. Satko et al. ACTA MATER, 2016, 107:377-89.